BEAM TESTS WITH S-BAND STANDING WAVE ACCELERATORS USING ON-AXIS COUPLERS

by
S.O. Schriber, E.A. Heighway and L.W. Funk

Atomic Energy of Canada Limited
Chalk River Nuclear Laboratories
Chalk River, Ontario, Canada

Abstract

Two electron S-band standing wave accelerators employing on-axis coupling cells have been designed and tested in the $\pi/2$ mode - one with 6 accelerating cells and the other with 21 accelerating cells. The maximum average accelerating gradient achieved with the 6-cell structure was 18 MeV/m. Rf drives to the accelerators were from pulsed magnetrons operating at 3 GHz.

Experimental measurements of the output beam characteristics including beam profile and energy measurements are presented as a function of electron gun injection energy, rf field levels and injection timing.

Introduction

For an accelerator where length costs are important, the advantage in using a side-coupled standing wave system operating in the $\pi/2$ mode has been demonstrated by LAMPF (1). When length costs are not so stringent, as for example, in short accelerators, the mechanical complexity of the side-coupled assembly can be avoided by using on-axis couplers. The accelerator naturally loses somewhat in shunt impedance in comparison ($\sim$ 6%).

A loop coupled equivalent circuit model indicates that the on-axis couplers should not create any problems with beam coupling interference when operated in the $\pi/2$ mode. A short 0.29 m six-cell S-band electron accelerator using on-axis couplers and operating in the $\pi/2$ mode was built to test such a system with beam loadings of up to 50% of the total rf drive.

Based on the success of the short system, a longer 21-cell accelerating system was built to see if any problems would arise with a long structure using on-axis coupling.

System Description

The accelerators were manufactured from OFHC copper segments obtained as forgings and were machined to the final cross section shown in Fig. 1. The accelerating structure was formed by brazing the segments together to form a bi-periodic system of alternate accelerating and pancake cells (Fig. 1). The accelerating cavity profile is similar to the Model K segments used by LASL (1,2). The accelerating cells were coupled to the pancake cells by two kidney shaped slots in the wall between the cells. In a given pancake cell wall these slots were positioned 180° to each other and at 90° to the slots in the neighbouring wall. This ensured that the second neighbour coupling of one accelerating cell to another was negligible. The first two (6 cell structure) or four (21 cell structure) cells were graded-β, the rest $\beta=1$.

Cell tuning was accomplished by the removal of small amounts of material from the nose region of each cell, the coefficients being 700 kHz/mill and 7 MHz/mill for the accelerating and pancake cells respectively. Each cell was tuned to within 500 kHz of the design frequency.

Rf power was coupled into the accelerator by cutting an iris in the wall of a central accelerating cell. Using a central cell ensured the flattest field distribution among the accelerating cells under beam loading. The iris cell had to be retuned during iris cutting using a special tool inserted along the accelerator axis.

To monitor rf fields, probes were mounted in the first, iris and last accelerating cells. These probes were mounted close to the outer perimeter of the cells in each case.

Vacuum was maintained in the accelerator by pumping through small slots in each of the pancake cells into a vacuum manifold along the length of the accelerator. A 60 ℓ/sec ion pump retained an operating pressure (with rf and beam on) of a few times 10^{-7} torr after rf conditioning but no vacuum bake-out.

The rf power system for the six cell accelerator was based on a 2.5 MW VC701E Varian magnetron operating at 2890 MHz. The pulse length was 4.5 μsec.

Isolation was provided by a four port circulator and tuning was effected by incorporating a variable mismatch and phase-shifter in the waveguide line to pull the magnetron. For the 21 cell accelerator a tuneable M5058 English Electric magnetron was used.

The electron gun was a triode of cylindrical Pierce geometry using a 2 kV pulsed mesh grid electrode for current control. The dc cathode potential was variable up to 100 kV. A 0.250" diameter directly heated dispenser cathode provided currents up to 300 mA peak. The beam pulse length was variable from 1.0 to 4.8 μsec and could be timed to coincide with any portion of the rf power pulse.

External electromagnetic focussing and steering were provided between the gun and accelerator.

The beam energy measurements, E and ΔE, employed a 30^{o} radially focussing bending magnet to obtain a momentum dispersed image at a 0.020" slit. The current transmitted through the slit was measured in a Faraday cup.

The beam profile was measured using a directly intercepting rotating helical wire scanner. The wire was 0.010" diameter tungsten wound to a 1" diameter helix with a 45^{o} pitch angle. Profiles in two perpendicular axes were obtained.

Accelerator Performance

For the short 6 cell accelerator the quantities chosen as monitors of accelerator performance were the beam energy E, defined as the most probable energy in the spectrum of the accelerated beam; the full width at half maximum of the output beam spectrum, ΔE; and the transmission T, defined as the ratio of accelerated current to electron gun current. These quantities were measured as functions of V_I, the gun dc cathode potential, (or injection voltage), V_{MOD}, the magnetron modulator voltage, before the pulse transformer, the current pulse length and τ, the time between the start of the rf power pulse and the start of the current pulse.

Figures 2 and 3 show plots of E and ΔE vs τ with V_{MOD} as a parameter. A minimum ΔE is observed for 2 μsec ≤ τ ≤ 3 μsec, which corresponds to the interval over which the combined effects of delivered rf power and beam loading serve to keep the field levels in the cells constant.

Figure 4 is a plot of E and ΔE as a function of V_I, with V_{MOD} as a parameter. Notice the relative insensitivity of E to changes in V_I, and the steady reduction of ΔE at all values of V_I as V_{MOD} increases. In addition, ΔE tends to increase with increasing V_I.

The highest value of E recorded in this series of measurements was 5 MeV, with V_{MOD} = 14 kV, V_I = 70 kV, a 1 μsec pulse length and τ = 4.0 μsec. The maximum electron energy of 5.15 MeV corresponds to a maximum gradient of 18 MV/m.

The accelerator transmission is plotted in Figs. 5 and 6, as a function of τ and V_I, respectively, with V_{MOD} as a parameter. These graphs show the strong dependence of T on V_{MOD} and τ, and the relatively weak dependence on V_I. The maximum transmission obtained for this accelerator was 32%.

An independent check of electron beam energy was carried out allowing the accelerated beam to strike a high-Z target. The dependence of bremsstrahlung dose rate on current and energy for this case has been experimentally established (Refs. 3 and 4).

$$D = 6.6 \times 10^{4} \; I \; E^{2.8}$$

where D = dose rate in Rads per minute at one metre
I = current in amps onto a gold target
E = beam energy in MeV.

The observed dose rate (measured on a calibrated ion chamber) for a 1 μsec long current pulse with τ = 3.5 μsec V_{MOD} = 14 kV, corresponded to E in the range 3.6 - 4 MeV. Under similar conditions with V_{MOD} = 13 kV, E lay in the range 3.3 - 3.7 MeV. Comparison with Fig. 2 shows good agreement.

For the 21-cell accelerator a low voltage diode gun replaced the triode. This was driven from the modulator in parallel with the M5058 magnetron. No independent variation of the injection voltage or beam pulse timing was therefore available. Figure 7 shows the performance of this accelerator as a function of injected beam current where the mean energy E and FWHM ΔE of the energy spectrum are both plotted.

At low injection currents, the most probable energy of 8.8 MeV corresponds to an average accelerating field of 8.8 MV/m,

limited by the power available from the magnetron at 1.7 MW. It is clear that the accelerator performance, as shown in the ΔE FWHM, is much improved at higher currents, being less than 200 keV above 150 mA injection. At 200 mA injection, with 35% transmission, the beam loading of 560 kW constitutes 33% of the available power.

Figure 8 shows that at low currents the energy spectrum is strongly double peaked whereas this feature is absent above 150 mA.

This indicates that the extra beam loading in the first accelerating cells is modifying the β-grading of the accelerator, and improving the phase acceptance at higher currents.

Beam profile measurements for the short accelerator indicated that no significant dependence on injection voltage or beam energy was present. The profile remained close to 3.5 mm FWHM and 8.0 mm FW 10% M. However when the beam pulse was shortened and timed to occur after complete rf filling of the accelerator the profile did improve to 3 mm FWHM and 7 mm FW 10% M.

For the longer accelerator the profile was distinctly broader than that for the short accelerator being 5 mm FWHM and 10 mm FW 10% M.

Conclusions

The first conclusion to be drawn from our work is that no serious problems were encountered using on-axis coupling cells in the two biperiodic accelerators tested in the $\pi/2$ mode. The beam currents transmitted agreed well with what is expected from phase losses alone based on both an impulse approximation and a point by point integration calculation using measured axial electric field distributions.

It is also clear that a high gradient (18 MV/m) can be tolerated in this type of structure and the limit here was in fact imposed on the structure by breakdown at the rf window in the waveguide line.

Two secondary conclusions emerged from these experiments. First, that the triode gun is a decided advantage since it allows variation in injection voltage and beam pulse length and timing variation. Second, the gas loading of the structure during beam on time was not excessive.

References

(1) E.A. Knapp, B.C. Knapp, J.M. Potter, Rev. Sci. Instr., 39, 979, 1968.

(2) H.C. Hoyt, D.D. Simmons, W.F. Rich; Rev. Sci. Instr. 37, 755, 1966.

(3) T.H. Martin, Sandia Laboratories Report SC-DR-69-240.

(4) A. Brynjolfsson, T.G. Martin; Int. J. App. Rad. and Isotopes 22, 29, 1971.

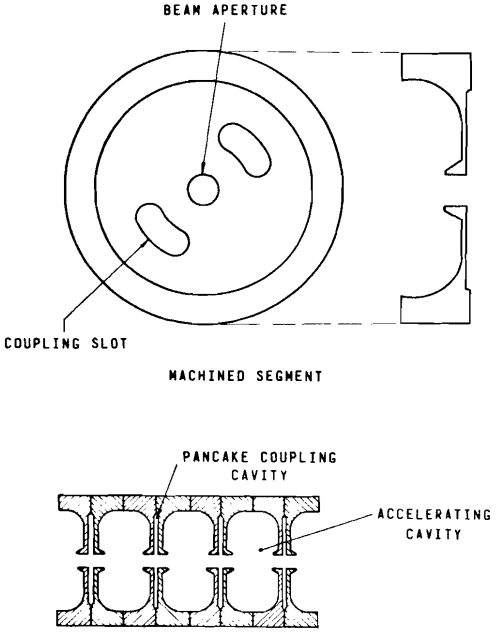

Fig. 1. Cross section of biperiodic cavity structure with pancake coupling cavities.

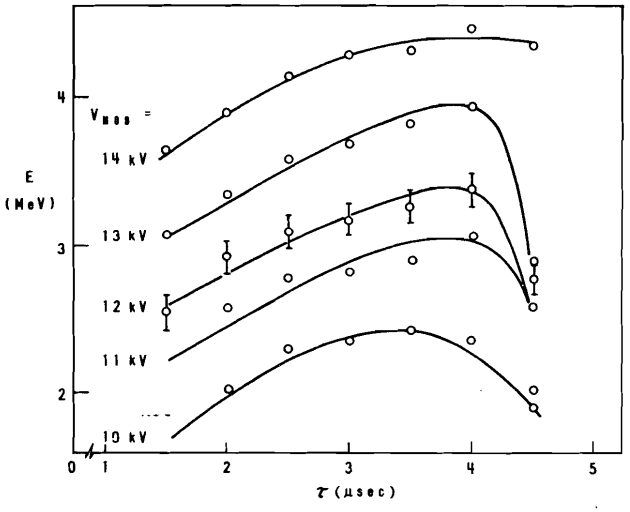

Fig. 2. Accelerator output energy as a function of the delay time between initiating the rf pulse and the electron beam pulse for different modulator voltage settings.

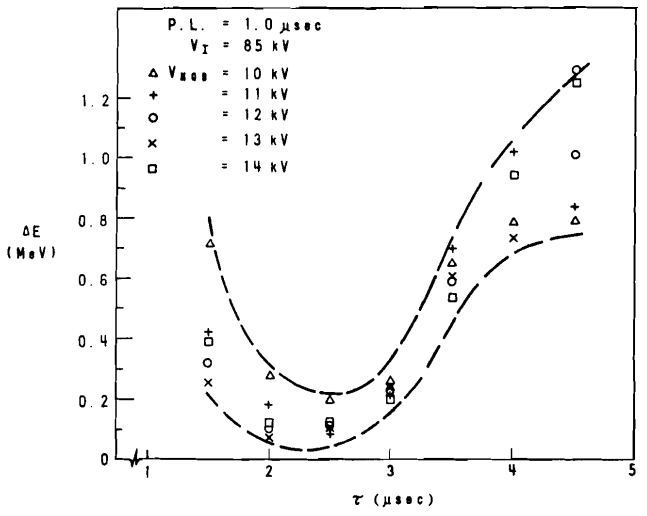

Fig. 3. FWHM energy spread of the output beam as a function of the delay time between initiating the rf pulse and the electron beam pulse for different modulator voltage settings.

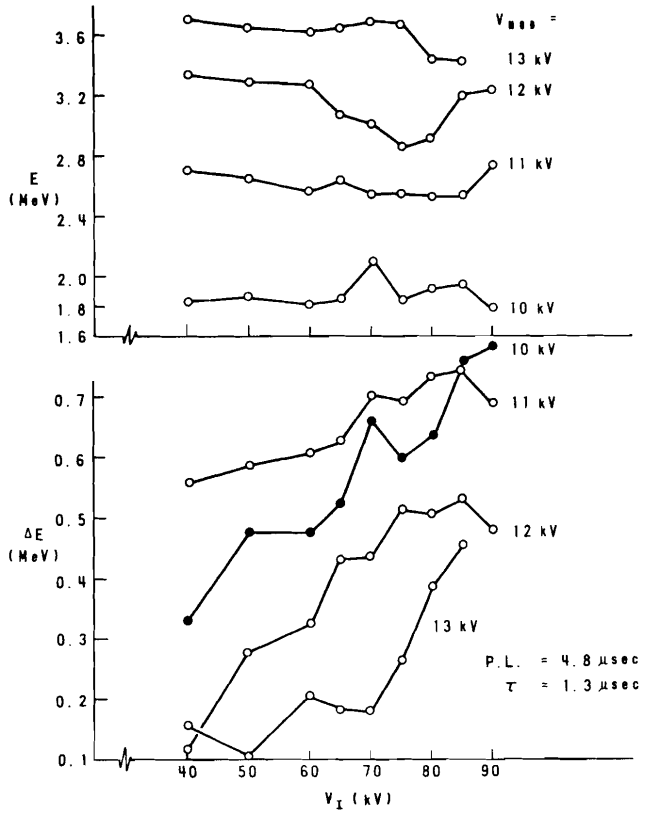

Fig. 4. Variation of the accelerator output energy and energy spread as a function of electron beam injection voltage for different modulator voltage settings.

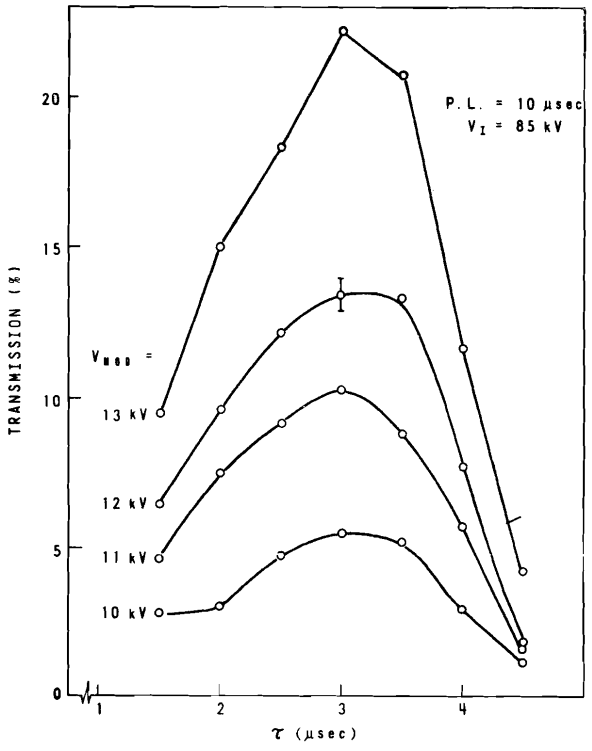

Fig. 5. Relative acceptance of the accelerator vs the delay time between initiating the rf pulse and the electron beam pulse for different modulator voltages.

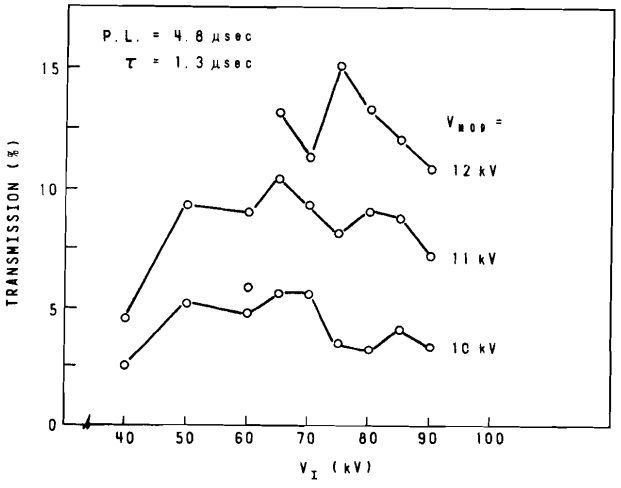

Fig. 6. Relative acceptance of the accelerator vs electron beam injection voltage for different modulator voltage settings.

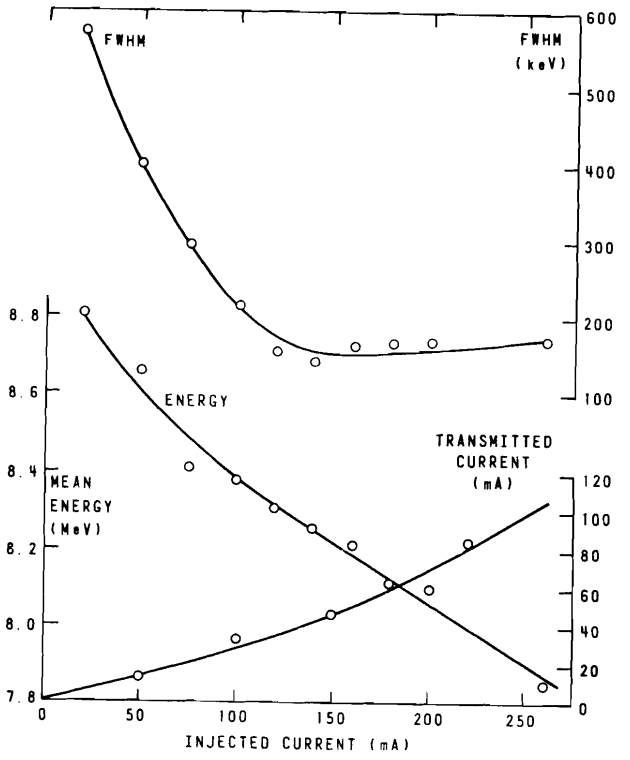

Fig. 7. FWHM energy spread of the output beam, output energy and transmitted current vs injected current for the 21 accelerating cell system.

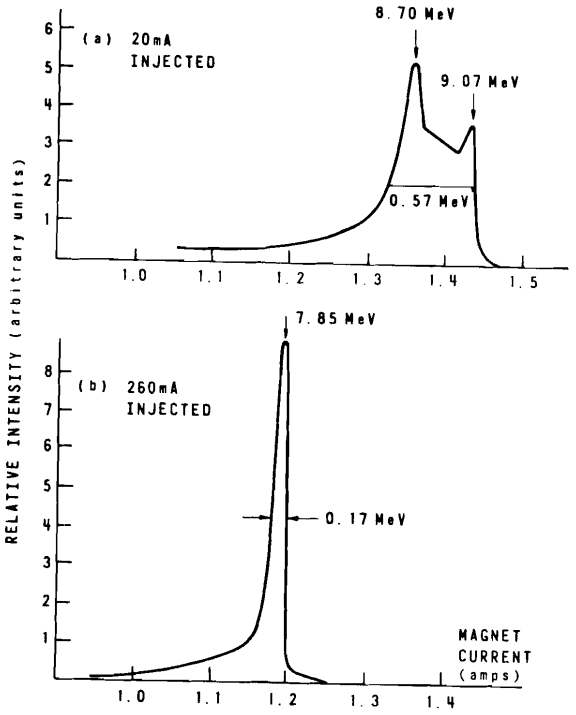

Fig. 8. Energy spectrum out of the 21 accelerating cell system for two different current injections.

DISCUSSION

Roger H. Miller, SLAC: What was the thickness of your pancake coupling cavity?

Schriber: It was 1/8 in.

Anselm Citron, Karlsruhe: With an 80 MV/m gradient, what were the highest fields occurring anywhere in the cavity? They must be of the order of 50 MV/m.

Schriber: Yes, it would be of that order. If you use the results from the LALA code, I think that if you compare the accelerating field to the highest surface field, the ratio is of the order of 5 to 7.

Citron: Did you observe any field emission?

Schriber: We did not really observe any field emission with the first system other than that you could notice a low radiation background. It was not like the values that were being quoted, i.e., 6R per hour at 30 cm. It was of the order of 2-4 mR off on the side.

H.A. Schwettman, Stanford Univ.: At what duty cycle were those radiation levels measured?

Schriber: At 0.1% duty cycle.

Schwettman: A few mR times a thousand equals a few R per hour.